Journal of Renewable Materials
DOI:10.32604/jrm.2020.011377
Article

Tech Science Press

Sawdust Short Fiber Reinforced Epoxidized Natural Rubber: Insight on Its Mechanical, Physical, and Thermal Aspects

O. S. Dahham[1], N. Z. Noriman[1,2,*], H. Jaya[1], R. Hamzah[1], M. U. Umar[2,3] and I. Johari[4]

[1]Advanced Polymer Research, Faculty of Chemical Engineering Technology, Universiti Malaysia Perlis (UniMAP), 02600 Pauh Putra Campus, Perlis, Malaysia
[2]School of Housing Building and Planning, Universiti Sains Malaysia, Minden, Penang, 11800, Malaysia
[3]JV Heritage Conservation & Technology Research Group (HEVEG), Penang, 11800, Malaysia
[4]School of Civil Engineering, Engineering Campus, Universiti Sains Malaysia, Nibong Tebal, Penang, 14300, Malaysia
*Corresponding Author: N. Z. Noriman. Email: niknoriman@unimap.edu.my
Received: 04 May 2020; Accepted: 30 June 2020

Abstract: In this work, Epoxidized natural rubber/sawdust short fiber (ENR-50/SD) composites at different fiber content (5, 10, 15 and 20 phr) and size (fine size at 60–100 μm and coarse size at 10–20 mm) were prepared using two-roll mill and electrical-hydraulic hot press machine respectively. Curing characteristics, water uptake, tensile, morphological, physical, and thermal properties of the composites were investigated. Results indicated that the scorch time and cure time became shorter whereas torque improved as SD content increase. Though the decline of tensile strength and elongation at break values, modulus, hardness and crosslinking density have shown enhancements with the increasing of SD content. The water uptake percentage of all samples has shown an increasing as SD content increase. However, the low SD content, particularly fine size have presented lower water uptake. The temperature of weight% loss (5 and 50 wt% loss) of 5 phr SD (low content) have recorded higher temperature compared to 20 phr SD (high content) in the rubber composites, which indicated higher thermal stability. The fine size of SD has recorded better overall properties than SD coarse size at same loading in the rubber composites.

Keywords: Epoxidized natural rubber; sawdust short fiber; cure characteristics; tensile properties; thermal stability

1 Introduction

Generally, natural rubber (NR) was extensively used as a base material to the products that require elastic characteristics as a requirement. Epoxidized Natural Rubber (ENR) is one of the natural elastomers having a good elasticity, which was used in the industrial area for several applications [1,2]. However, some of rubber products require the stiffness along with flexibility in certain applications, this can be achieved by adding filler to the rubber with certain size, amount and surface chemistry to suit the required applications. Several researches could be found in the literature study the influences of commercial fillers such as silica, carbon black, calcium carbonate and others on the properties of rubber/commercial fillers composites [3–9]. Furthermore, rubber/commercial filler composites were also used in rubber industry [10,11].

In recent years, the addition of natural fillers, particularly natural fibers into polymeric materials have attracted the attention of researchers, scientists and technologists and several studies were conducted in this field [12–14]. Natural fibers were used as a replacement for conventional fibers (glass, aramid, carbon and others) in numerous applications due to their advantages, such as lightweight, acceptable mechanical properties, environmentally friendly and abundance in nature. The development of natural fiber reinforced rubber has made available polymers that are harder than aluminum and stiffer than steel [15]. However, some of natural fiber/rubber composites properties, such as mechanical, rheological, physical and thermal properties can be effected by several factors, such as fiber-polymer volume fraction, fiber orientation, fibers aspect ratio, dispersion level, fiber–polymer adhesion, mixing time and processing temperature. Sareena et al. assessed the ability of coconut shell powder to be used as novel filler in natural rubber. The results shown that the vulcanizate at low content of coconut shell powder (10 phr) had better mechanical properties. However, the composites with high content of coconut shell powder (40 phr) gave better hardness. In addition, incorporation of coconut shell powder into rubber shown composites with improved thermal properties [16]. Other researcher, such as Ismail et al. investigated the influence of different oil palm wood flour (OPWF) content and size on curing characteristics and mechanical properties of OPWF/ENR composites. The results suggest that the cure characteristics, tear strength, modulus and hardness are improved as OPWF content increase in ENR. Despite the reduction of tensile strength and elongation at break, smaller particle size of OPWF showed better overall properties [17]. Our previous research investigated the effects of different natural fiber (rice husk) loading and size on the properties of epoxidized natural rubber/rice husk composites. It is found that the addition of rice husk into epoxidized natural rubber improved the cure characteristic and physical properties of the composites. However, the high amount of rice husk showed negative effect on the tensile strength and flexibility of the composites [18]. There are limited works conducted in sawdust short fiber with natural rubber. Furthermore, these limited works didn't give a complete assignment on the sawdust short fiber/natural rubber composites. Consequently, the main objective of this work is to give an extensive study of the sawdust short fiber reinforced epoxidized natural rubber. This extensive study covered cure characteristic, tensile, physical, morphological and thermal properties.

2 Experimental Details

2.1 Materials

Epoxidized natural rubber at 50 % epoxide content (ENR-50) was used as a main material in this work. ENR-50 was obtained from Rubber Research Institute of Malaysia (RRIM). Sawdust short fibers (SD) were used as natural filler. SD fibers were obtained from Bernas Malaysia Sdn. Bhd., Simpang Empat, Perlis, Malaysia. The other materials and chemicals, such as vulcanizing agent (sulfur), inorganic activator (zinc oxide), organic activator (stearic acid), accelerator (N-cyclohexyl-2-benzothiazole sulfonamide) and solvent (toluene) were purchased from Anchor Chemical Co., (M) Ltd. All the ingredients and formulations used in this work are listed in Tab. 1.

Table 1: The formulation of ENR-50/SD composites

Ingredients	PHR				
	R0	R05	R10	R15	R20
ENR-50	100	100	100	100	100
ZnO	5	5	5	5	5
Stearic Acid	2	2	2	2	2
CBS	1	1	1	1	1
Sulfur	2	2	2	2	2
SD fs Cs	0	5	10	15	20

Where fs is Sawdust—fine size, Cs is Sawdust—Coarse size, and PHR refer to parts per hundred rubber, which is a measure used by rubber chemists to describe the amount of certain ingredients are required, particularly in pre-vulcanization rubber.

2.2 Samples Preparations, Cure Characteristics and Vulcanization

First, SD were collected and dried under sun exposure for 2 days before use. Different content (5, 10, 15 and 20 phr) and different sizes of SD (60–100 μm and 10–20 mm) were obtained using Crusher model RT34 (Chyun Industrial Co., Ltd.) and lab sieves respectively. The Mastersizer (Type E) was used to analyze the particle size distribution of SD fine size, as shown in Fig. 1. Two-roll mill model X (S) K - 160 × 320 was utilized for rubber mastication and mixing with other ingredients based on ASTM D 3184-89. Cure characteristics were analyzed using a Monsanto Moving Die Rheometer model (MDR 2000) according to ASTM D 2240-93 at 160°C temperature. Electrical-hydraulic hot press machine was utilized to compression accordingly to respective cure time at 160°C temperature with pressure of 294199.5 Pascals m^{-2}.

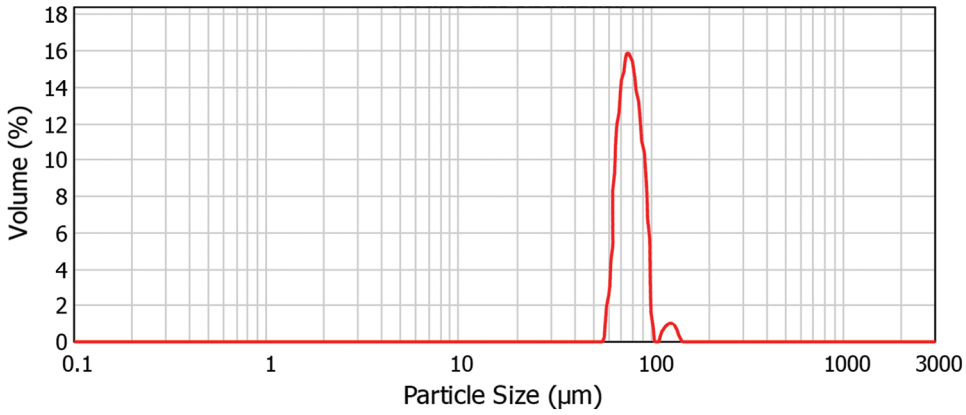

Figure 1: Particle size distribution of sawdust (SD) fiber–fine size

2.3 Tensile Properties

Wallace die cutter was used based on ASTM D 638 to form a dumbbell shape samples for tensile test purpose. Tensile test was conducted using Universal Testing Machine model (Instron 5582) based on ASTM D412. The exposed samples were pulled at 500 mm/min crosshead speed with 25°C temperature. The readings of tensile strength (Ts), elongation at break (E_b), and modulus at 100% elasticity (M100) were recorded.

2.4 Morphological Properties

The tensile fracture surface of selected samples was analyzed using scanning electron microscopy (SEM) model (JEOL JFC6460LA). The fracture surface for dumbbell samples after tensile test were collected and then an extremely thin layer of palladium (1.5–3 nm) was selected for samples coating using sputter coater machine to avoid poor resolution and electrostatics charging during analyzing.

2.5 Water Uptake

The test of water uptake was conducted by immersing the prepared samples in distilled water at Temperature 25°C. The vacuum oven was used 6 hours at 100°C in order to dry the samples till a constant weight was reached prior to immersion in water in thermostated vessels at ambient temperature. The weight gains after exposure were reported by weighing the samples on an electronic balance with 1 mg accuracy (Model BS224S Sartorius AG, Germany). The moisture absorption at a certain time t, Mt (%) was calculated by Eq. (1).

$$Mt = 100 \times (w_t - w_o)/w_o \tag{1}$$

where w_o and w_t are original dry weight and weight after exposure, respectively.

2.6 Physical Properties

Hardness measurement of the samples was performed according to ASTM D 2240-81 using a Shore A durometer. Hardness value of each sample was obtained from three different points distributed on the tested sample surface and the average value was determined. The swelling test was carried out using toluene solvent according to ASTM D471-79. Vulcanized rubber samples were cut into (30 mm × 5 mm × 2 mm) dimension and weighed to calculate the initial weight. Each sample was immersed in a vessel containing toluene (30 mL) at 25°C temperature separately and reserved in a dark place to avoid oxidation. Samples were kept about 72 hours in a close glass vessel to prevent toluene evaporation. After samples immersing, swollen samples were wiped and directly weighed again to calculate the weight after swelling. The swelling percentage of the samples was calculated by using Eq. (2).

$$S = 100 \times (w_s - w_o)/w_o \tag{2}$$

where w_o and w_s are original dry weight and weight after swelling exposure, respectively. The swelling data were used for crosslinking density calculations using Flory Rehner equations [19].

2.7 Thermal Properties

Thermogravimetric analysis (TGA) of the selected samples was conducted with the TGA analyzer model Perkin-Elmer Pyris 6. The samples, which weighed about 15 mg, scanned from 30°C to 820°C at 50 mL/min nitrogen airflow and 20 °C/min heating rate.

3 Results and Discussion

3.1 Cure Characteristics

The curing characteristics, such as scorch time (t_2), cure time (t_{90}), minimum torque (M_L) and maximum torque (M_H) of SD filled ENR-50 were investigated and shown in Tab. 2 respectively. It is obvious that t_2 and t_{90} decreased with increasing SD content in ENR-50 matrix. The cure improvement of ENR-50/SD composites as SD content increased could be attributed to the filler-related parameters such as particle size, metal oxide content, surface area, surface reactivity and moisture content [20]. M_L is directly proportional to the viscosity of the uncured rubber, which increased as SD content increased in the rubber composites. Therefore, the processability became more difficult. M_H also increased with increasing SD contents in the rubber composites. The increment in the M_H with SD content is due to the existence of more SD that gave more restriction to the deformation and consequently improved the stiffness of the rubber composites. At same SD loading, the SD fine size exhibited better overall cure characteristics than SD coarse size. Based on Ishak and Bakar research, the smaller particle size of filler means larger surface area and greater filler-rubber interaction. Therefore, lower time of curing and higher restriction to molecular movement of the macromolecules is expected [21].

Table 2: Cure characteristics of ENR-50/SD composites at different SD loading and size

	SD	t_2 (min)	t_{90} (min)	M_L (dNm)	M_H (dNm)
R0	Control	2.4	9.8	4.64	19.9
R05	fs	0.83	6.20	6.56	28.4
	cs	1.21	6.62	5.2	26.7
R10	fs	0.66	6.00	9.89	30.1
	cs	0.94	6.25	8.39	28.5
R15	fs	0.39	5.13	13.04	34.8
	cs	0.61	5.49	11.91	30.3
R20	fs	0.26	4.97	16.03	37.2
	cs	0.42	5.37	14.1	33.0

3.2 Tensile Properties

The variations of tensile strength (Ts), elongation at break (Eb) and modulus at 100% elasticity (M100) in ENR-50/SD composites at different SD loading and size are shown in Figs. 2–4 respectively. It can be seen obviously that Ts and E_b values of the composites decreased as SD increased. The gradual declining of Ts and E_b was due to the increased agglomeration of the SD fiber in the ENR-50 matrix and SD filler, which in turn led to decrease the stress transmission from matrix to fiber [22,23]. Nevertheless, the fine size of SD exhibited higher Ts and E_b values than coarse size of SD at same loading in the composite. This was attributed to the high distribution of SD fine size in ENR-50 matrix, which increased fiber/matrix bonding. This matter was proved in the morphology section (Fig. 5). M100 in Fig. 3 displays opposite trend than Ts and E_b, which increased linearly as SD content increased in the rubber composites. It is believed that the increasing of SD content, particularly SD fine size have increased the stiffness and reduced the flexibility of the rubber composites, consequently M100 was improved.

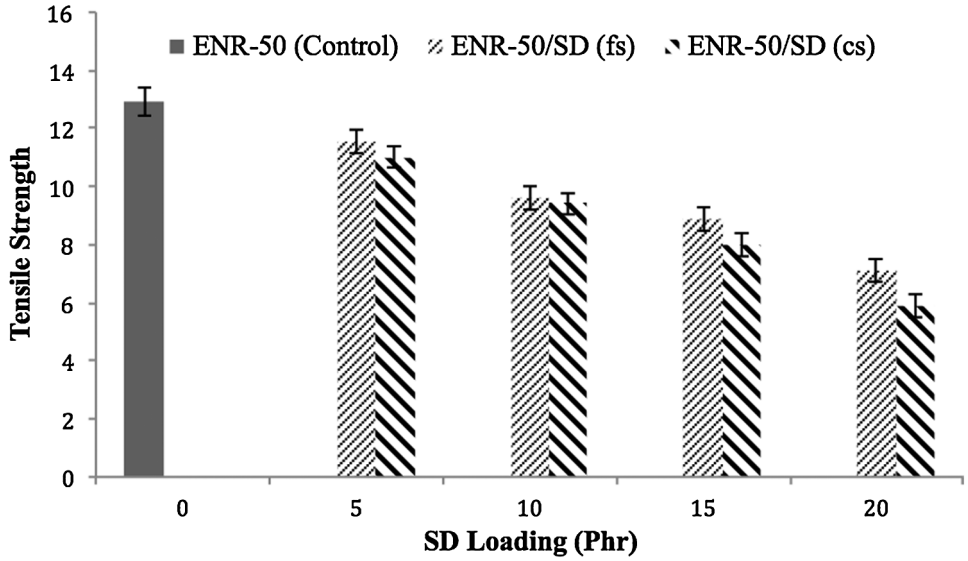

Figure 2: Variation of tensile strength of ENR-50/SD composites at different SD loading and size

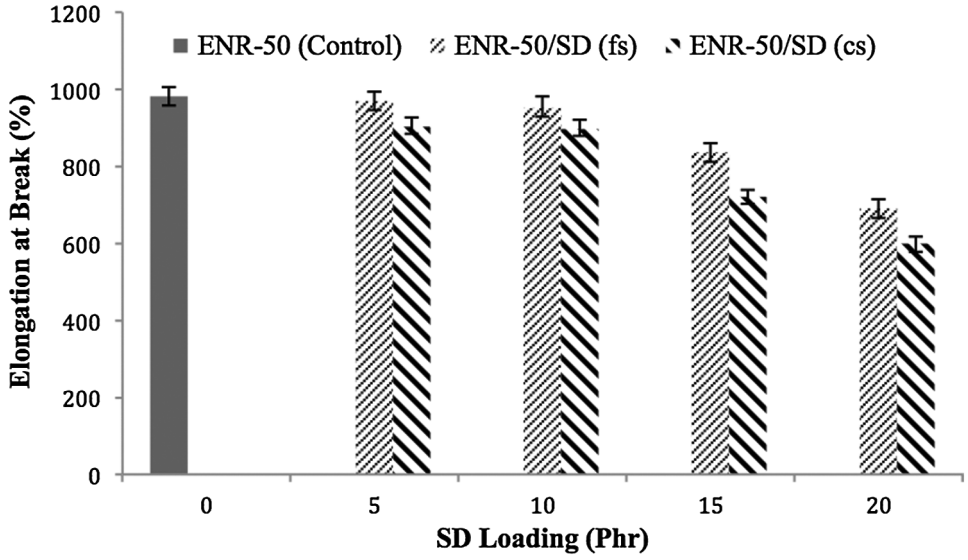

Figure 3: Variation of elongation at break of ENR-50/SD composites at different SD loading and size

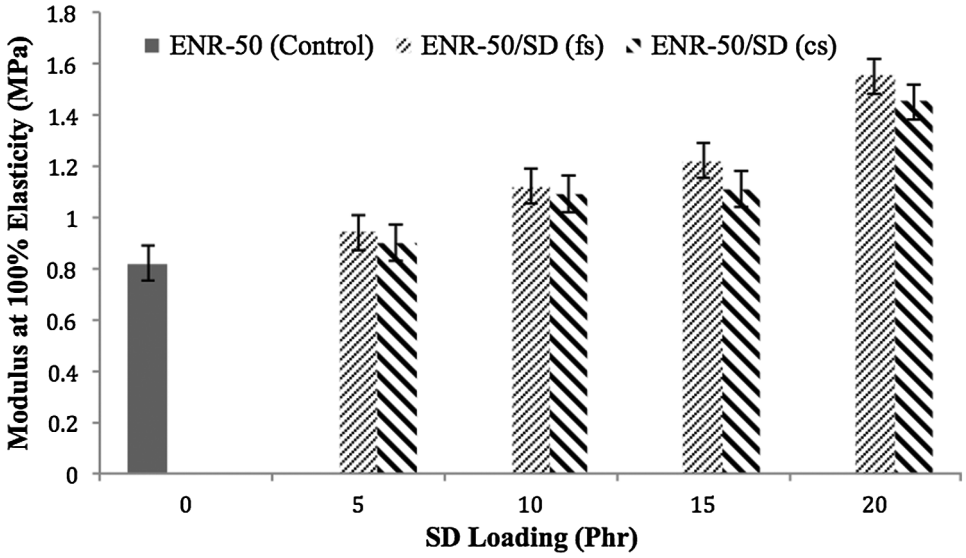

Figure 4: Variation of modulus at 100% elasticity of ENR-50/SD composites at different SD loading and size

3.3 Morphology

The scanning electron microscopy (SEM) of the tensile fractured surface of ENR-50 control, ENR-50/SD (5 phr-fs), ENR-50/SD (5 phr-cs), ENR-50/SD (20 phr-fs) and ENR-50/SD (20 phr-cs) with 500× magnification were illustrated in Figs. 5a–5e respectively. According to the result of Ts recorded in Fig. 1 and the fracture surface images of the lower SD content, particularly ENR-50/SD (5 phr-fs) in Fig. 6b, several tearing lines appeared on the tensile fracture surface indicating that the sample needs more energy to break the matrix. This phenomenon indicated that the 5 phr SD was lower tendency of agglomeration than 20 phr SD, which strongly bonded with the ENR-50 matrix and produced a high adhesion bonding. The higher SD content in the rubber composites, particularly ENR-50/SD (20 phr-cs) presented different behavior than lower SD content, which exhibited SD agglomerations in ENR-50 matrix and formed a rough surface (Fig. 6e). This agglomerations reduced the SD surface area which caused breakages and pull out of the SD and holes occurred [24,25].

3.4 Water Uptake

Fig. 6 shows the water uptake of ENR-50/SD composites at different SD loading and size. It is clearly observed that the water uptake of the composites has increased with increasing immersion time and SD loading in the composites. Similar observations were found by other researchers [26]. All samples have shown a similar trend of water uptake. It is also observed a high water uptake by the samples followed by a gradual increase until an equilibrium stage was reached at the end of experiment (the 30^{th} day). SD has a hydrophilic nature, this is due to the hydroxyl groups (OH) existing in cellulose that is capable to produce hydrogen bonds between SD and water [27]. Also, the presence of micro-cracks, pores, lumens and/or voids in the rubber matrix, along with flaws and gaps at the interfaces, may increase the water uptake by natural fibre polymer composites [26,28].

According to Fig. 6, the results suggest that the water uptake percentage of the samples increased with increase of SD loadings. When the SD loadings increase, the number of hydrogen bonds formed between water molecules and SD fibers also increase along with the number of OH groups existing in the

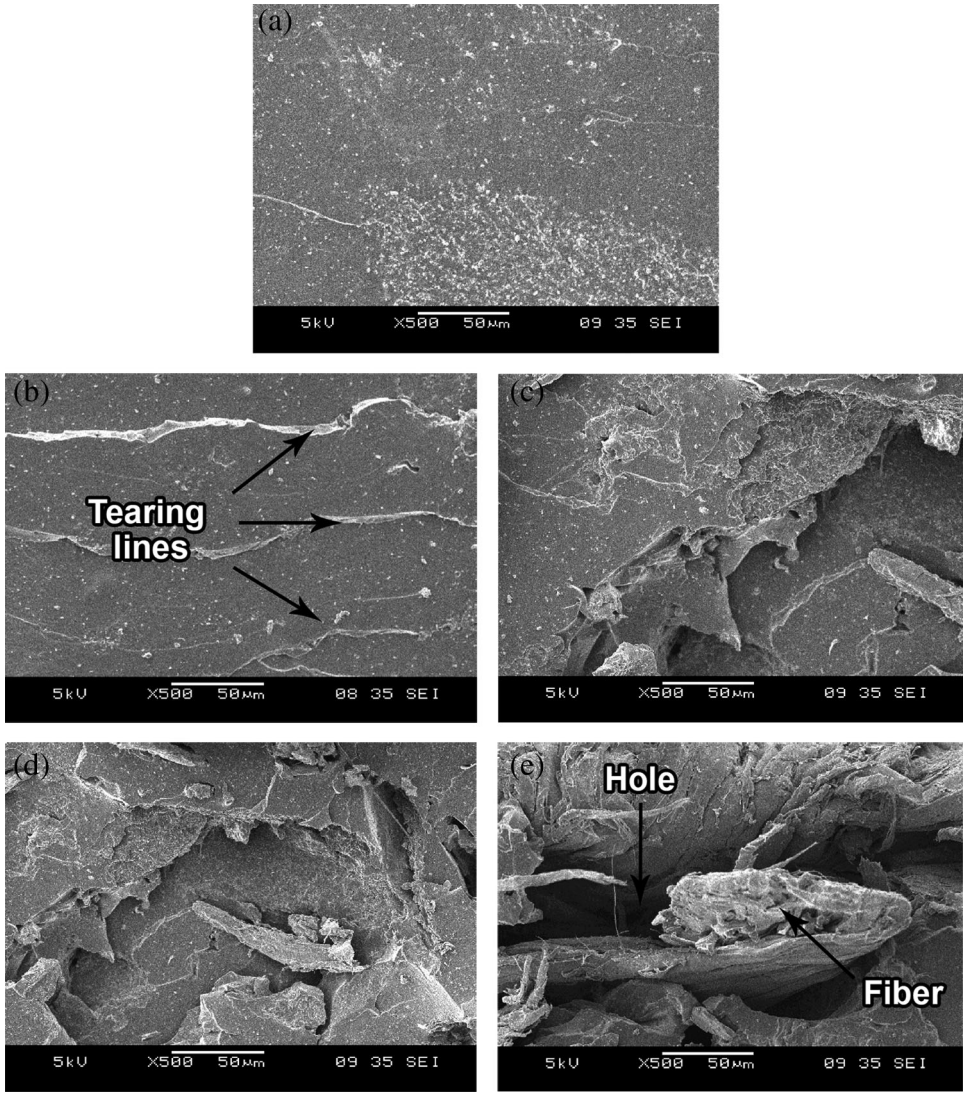

Figure 5: SEM of tensile fracture surface of (a) ENR-50 control and ENR-50/SD composites at SD (b) 5 phr-fs, (c) 5 phr-cs, (d) 20 phr-fs and (e) 20 phr-cs, 500× magnification

cellulose. Also, higher percentage of water uptake by samples with higher SD loading was due to the increasing number of voids between SD fiber and rubber matrices. At same SD loading, the samples with a smaller SD size has shown a lower percentage of water uptake as compared to the samples with coarser SD size. This is due to the lower number of voids between SD fiber (fine size) and rubber matrices, which in turn restricted the penetration of water molecules in the samples.

Furthermore, it can be clearly observed two different stages of weight gain due to moisture penetration into the ENR-50/SD composites, as shown in Fig. 6. The first stage refers to the water molecules diffusion inside the micro-gaps between the polymer chains, The second stage refers to the capillary transport of water molecules into the flaws and gaps formed at the SD fiber interface and polymer matrix due to incomplete impregnation and wettability and also due the water molecules diffusion into the micro-cracks created in the matrix during the compounding process of the samples [27].

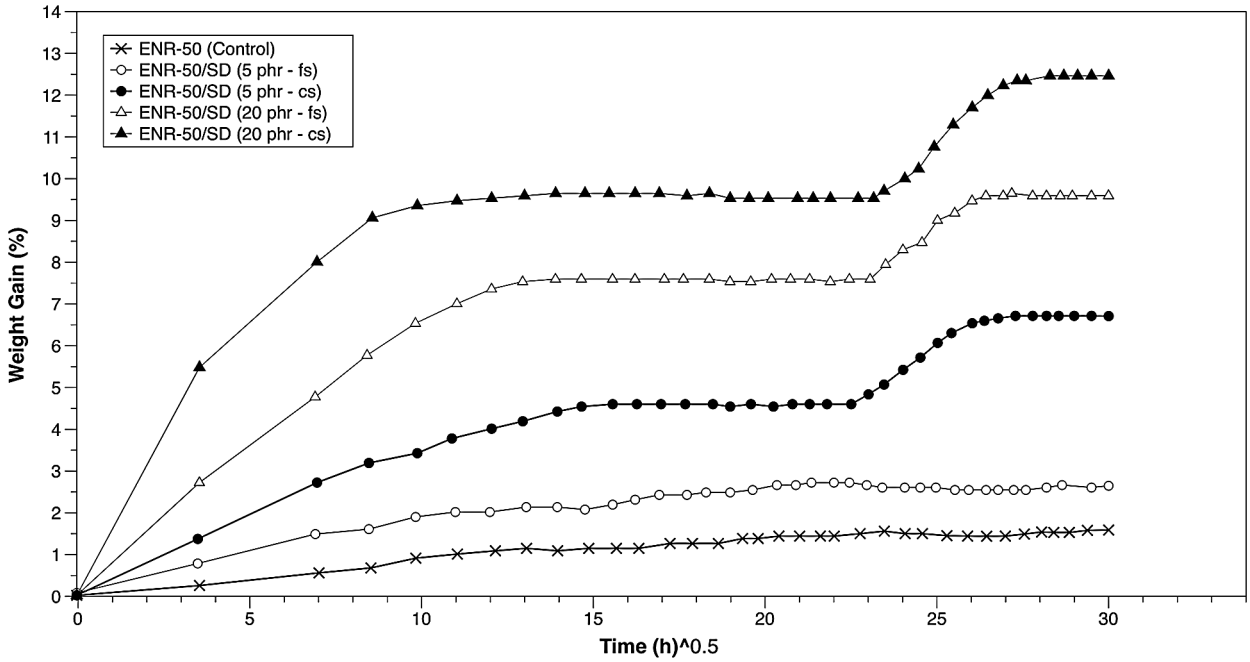

Figure 6: The percentage of weight gain of ENR-50/SD composites at different SD loading and size

3.5 Physical Properties

The effects of SD content and size on the hardness, swelling percentage and crosslinking density are shown in Figs. 7–9 respectively. The hardness values were improved when SD increased in ENR-50/SD composites. The gradual rising of the hardness explained the increasing of the rubber composites rigidity and the improvement of the crosslinking density (Fig. 9). The swelling percentage decreased with increasing SD content due to the decreasing of voids in the rubber composites, which in turn led to reduce the penetration of toluene solvent inside rubber composites [24,29]. The addition of SD fine size presented higher hardness and crosslinking density values than SD coarse size at same SD loading. This might be due to the larger surface area of the SD fine size than SD coarse size that obtained better interaction with ENR-50 at any loading.

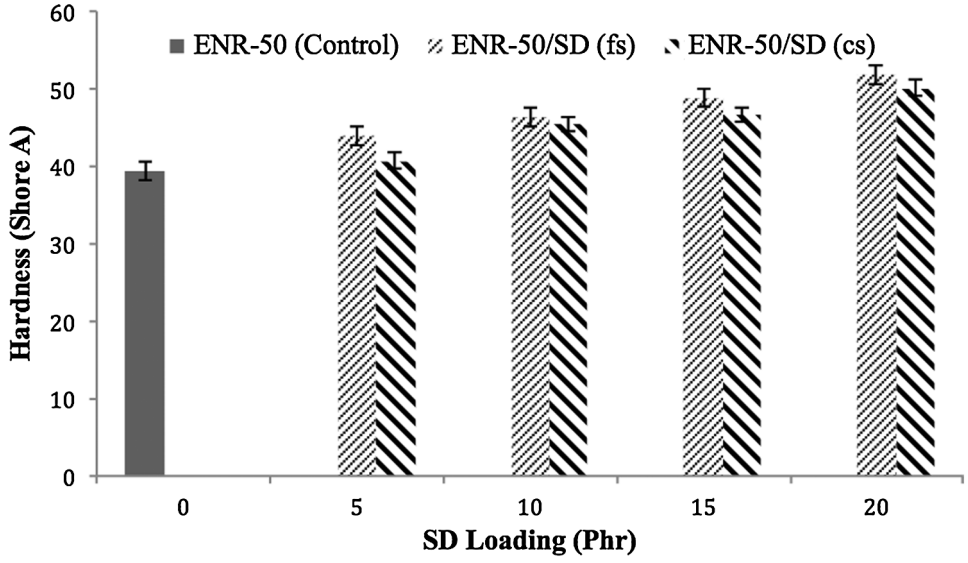

Figure 7: Variation of hardness of ENR-50/SD composites at different SD loading and size

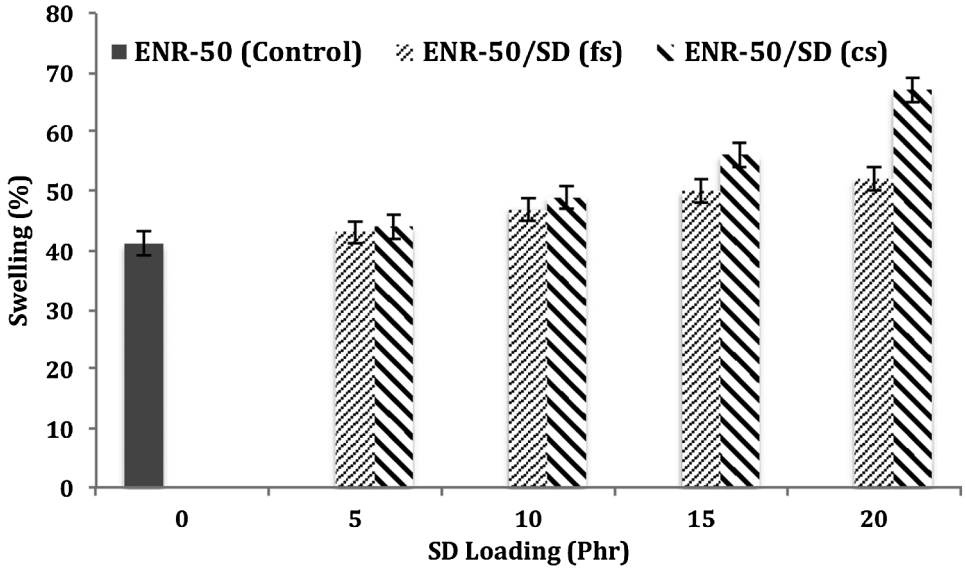

Figure 8: Variation of swelling percentage of ENR-50/SD composites at different SD loading and size

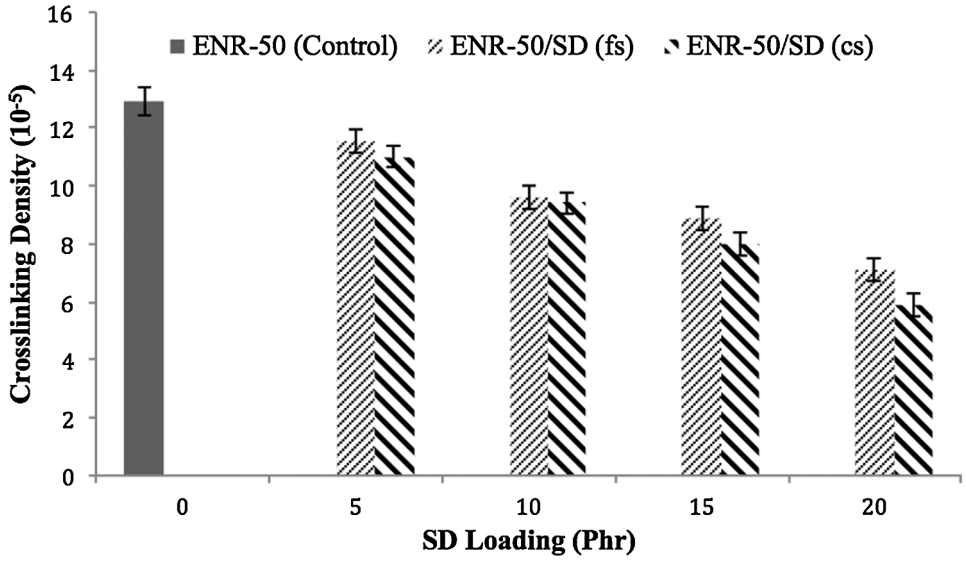

Figure 9: Variation of crosslinking density of ENR-50/SD composites at different SD loading and size

3.6 Thermal Properties

The results of thermogravimetric analysis (TGA) and derivative thermogravimetric analysis (DTG) of ENR-50 control, ENR/SD (5 phr-fs), ENR-50/SD (5 phr-cs), ENR/SD (20 phr-fs) and ENR/SD (20 phr-cs) are shown in Fig. 10 and Tab. 3 respectively. TGA of two different loading (5 and 20 phr) and size (fs and cs) of SD filled ENR-50 presented degradation steps, which characterized the decomposition of the composites. The onset degradation step was recorded at the temperature of 5 wt% loss ($T_{5\%}$), which was 361°C for ENR/SD (5 phr-fs), 360°C for ENR/SD (5 phr-cs), 358°C for ENR/SD (20 phr-fs), 357°C for ENR/SD (20 phr-cs) and 253°C for ENR-50 control. In conjunction with ($T_{5\%}$), the temperature of 50 wt% loss ($T_{50\%}$) recorded 459°C for ENR/SD (5 phr-fs), 457°C for ENR/SD (5 phr-cs), 455°C for ENR/SD (20 phr-fs), 453°C for ENR/SD (20 phr-cs) and 445°C for ENR-50 control. The high

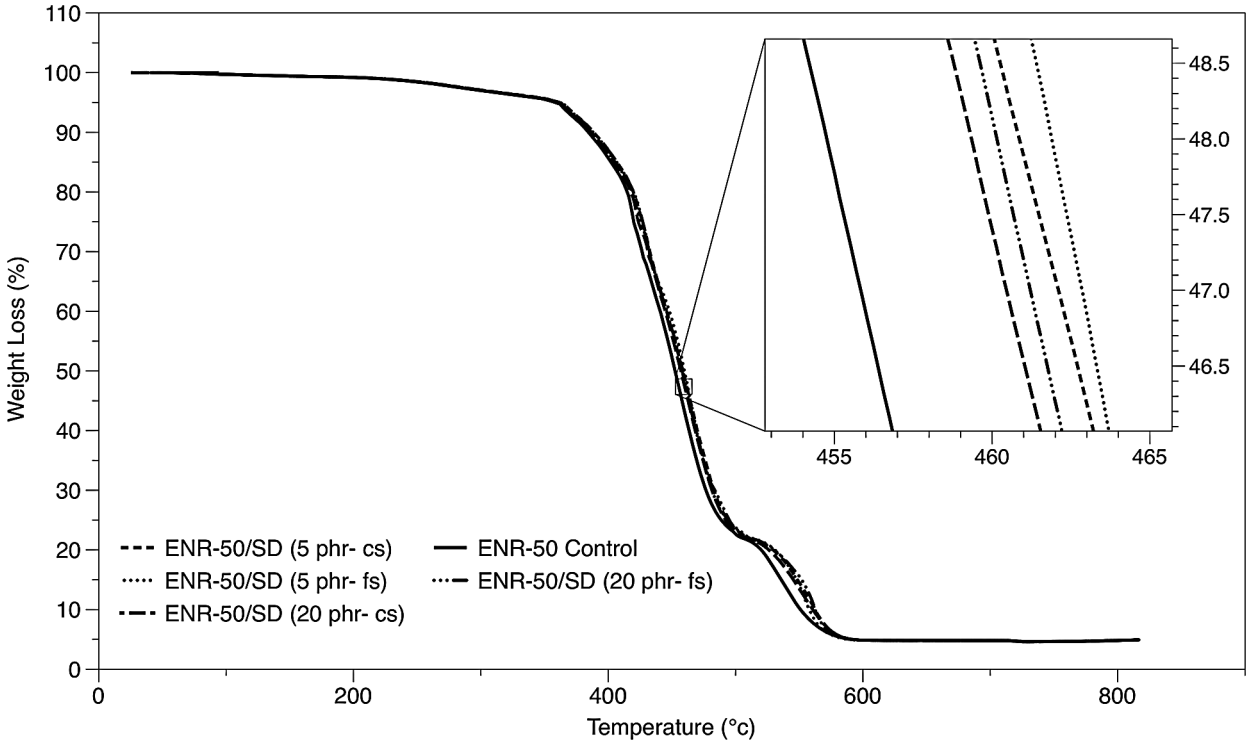

Figure 10: TGA thermograms of ENR-50/SD composites

Table 3: Experimental data of TG and DTG of ENR-50/SD composites

Rubber composites	($T_{5\%}$)°C	($T_{50\%}$)°C	($T_{max\ dec}$)°C	DTG peak%/min^{-1}
ENR-50 control	253	445	440	−0.092
ENR-50/SD (5 phr-fs)	361	459	458	−0.158
ENR-50/SD (5 phr-cs)	360	457	454	−0.149
ENR-50/SD (20 phr-fs)	358	455	453	−0.123
ENR-50/SD (20 phr-cs)	357	453	450	−0.114

temperature of ENR/SD (5 phr), particularly fine size referred to the high thermal stability, which might due to the higher adhesion between ENR-50 and SD low content/fine size that reduced ENR-50 main chains breakdown compared to higher SD content/coarse size [29,30].

The DTG thermograms revealed that the DTG peak of ENR-50/SD (5 phr-fs) at −0.158%/min^{-1} was lower value than ENR-50/SD (5 phr-cs) at −0.149%/min^{-1}, ENR-50/SD (20 phr-fs) at −0.123%/min^{-1}, ENR-50/SD (20 phr-cs) at −0.114%/min^{-1} and ENR-50 control at −0.092%/min^{-1}. Additionally, the temperature at maximum peak decomposition ($T_{max\ dec}$) of ENR-50/SD (5 phr-fs) at 458°C exhibited higher temperature than ENR-50/SD (5 phr-cs) at 454°C, ENR-50/SD (20 phr-fs) at 453°C, ENR-50/SD (20 phr-cs) at 450°C and ENR-50 control at 440°C (Tab. 3). The lower DTG peak and higher ($T_{max\ dec}$) of ENR-50/SD (5 phr), particularly fine size referred to the slower degradation process than other ENR-50/SD composites [31]. The thermal stability of ENR-50/SD composites at any SD loading and size was higher than ENR-50 control. The positive impact of SD on the thermal stability of ENR-50 may be

explained by reduction of ENR-50 phase mobility in the vicinity of SD. The reduction of ENR-50 chain mobility might lead to slower diffusion of degradation products from the system [32,33].

4 Conclusion

In conclusion, the increasing of SD content into ENR-50 has reduced the scorch and cure time while increased the torque. Despite the deterioration of tensile strength of the rubber composites when SD content increase, the physical properties and modulus were improved. In contrast, the lower SD content exhibited higher thermal stability and slower degradation process than higher SD content. At same loading, the fine size of SD presented better overall properties than coarse size in the rubber composites due to the high adhesion bonding between SD fine size and ENR-50 matrix, which was proven by SEM section.

Acknowledgement: The authors would like to thank Universiti Malaysia Perlis-Malaysia, for providing us all the facilities to complete this work successfully.

Funding Statement: The authors received no specific funding for this study.

Conflicts of Interest: The authors declare that they have no conflicts of interest to report regarding the present study.

References

1. Baker, C. S. L., Gelling, I. R., Newell, R. (1985). Epoxidized natural rubber. *Rubber Chemistry and Technology, 58 (1),* 67–85. DOI 10.5254/1.3536059.
2. Hamzah, R., Bakar, M. A., Dahham, O. S., Zulkepli, N. N., Dahham, S. S. (2016). A structural study of epoxidized natural rubber (ENR-50) ring opening under mild acidic condition. *Journal of Applied Polymer Science, 133(43),* 184. DOI 10.1002/app.44123.
3. Chan, C. M., Wu, J., Li, J. X., Cheung, Y. K. (2002). Polypropylene/calcium carbonate nanocomposites. *Polymer, 43(10),* 2981–2992. DOI 10.1016/S0032-3861(02)00120-9.
4. Xu, T., Jia, Z., Luo, Y., Jia, D., Peng, Z. (2015). Interfacial interaction between the epoxidized natural rubber and silica in natural rubber/silica composites. *Applied Surface Science, 328,* 306–313. DOI 10.1016/j.apsusc.2014.12.029.
5. George, K. M., Varkey, J. K., Thomas, K. T., Mathew, N. M. (2002). Epoxidized natural rubber as a reinforcement modifier for silica-filled nitrile rubber. *Journal of Applied Polymer Science, 85(2),* 292–306. DOI 10.1002/app.10658.
6. Tangboriboon, N., Rortchanakarn, S., Petcharoen, K., Sirivat, A. (2015). Effects of foaming agents and calcium carbonate on thermo-mechanical properties of natural rubber foams. *Polimeri, 35*.
7. Gupta, M. K., Srivastava, R. K. (2016). Mechanical properties of hybrid fibers-reinforced polymer composite: A review. *Polymer-Plastics Technology and Engineering, 55(6),* 626–642. DOI 10.1080/03602559.2015.1098694.
8. Surya, I., Ismail, H. (2016). The effect of the addition of alkanolamide on properties of carbon black-filled natural rubber (SMR-L) compounds cured using various curing systems. *Polymer Testing, 50,* 276–282. DOI 10.1016/j.polymertesting.2016.01.014.
9. Laftah, W. A., Hashim, S. (2014). The influence of plant natural fibers on swelling behavior of polymer hydrogels. *Journal of Composite Materials, 48(5),* 555–569. DOI 10.1177/0021998313476323.
10. Sengloyluan, K., Sahakaro, K., Dierkes, W. K., Noordermeer, J. W. (2014). Silica-reinforced tire tread compounds compatibilized by using epoxidized natural rubber. *European Polymer Journal, 51,* 69–79. DOI 10.1016/j.eurpolymj.2013.12.010.
11. Thomas, S., Stephen, R. (2010). *Rubber nanocomposites: preparation, properties, and applications*. John Wiley & Sons.
12. Thakur, V. K., Thakur, M. K., Gupta, R. K. (2014). Raw natural fiber-based polymer composites. *International Journal of Polymer Analysis and Characterization, 19(3),* 256–271. DOI 10.1080/1023666X.2014.880016.

13. Jawaid, M. H. P. S., Khalil, H. A. (2011). Cellulosic/synthetic fibre reinforced polymer hybrid composites: A review. *Carbohydrate Polymers, 86(1),* 1–18. DOI 10.1016/j.carbpol.2011.04.043.
14. Balaed, K., Noriman, N. Z., Dahham, O. S., Sam, S. T., Hamzah, R. et al. (2016). Characterization and properties of low-linear-density polyethylene/Typha latifolia composites. *International Journal of Polymer Analysis and Characterization, 21(7),* 590–598. DOI 10.1080/1023666X.2016.1183336.
15. Jacob, M., Thomas, S., Varughese, K. T. (2004). Natural rubber composites reinforced with sisal/oil palm hybrid fibers: Tensile and cure characteristics. *Journal of Applied Polymer Science, 93(5),* 2305–2312. DOI 10.1002/app.20696.
16. Sareena, C., Ramesan, M. T., Purushothaman, E. (2012). Utilization of coconut shell powder as a novel filler in natural rubber. *Journal of Reinforced Plastics and Composites, 31(8),* 533–547. DOI 10.1177/0731684412439116.
17. Ismail, H., Rozman, H. D., Jaffri, R. M., Ishak, Z. M. (1997). Oil palm wood flour reinforced epoxidized natural rubber composites: The effect of filler content and size. *European Polymer Journal, 33(10–12),* 1627–1632. DOI 10.1016/S0014-3057(97)00020-7.
18. Dahham, O. S., Noriman, N. Z., Sam, S. T., Al-Samarrai, N. M., Shayfull, Z. et al. (2016). The influence of rice husk fiber on the properties of epoxidized natural rubber/rice husk compounds. *MATEC Web of Conferences, 78,* 01075. EDP Sciences.
19. Flory, P. J., Rehner, J. Jr. (1943). Statistical mechanics of cross-linked polymer networks I. Rubberlike elasticity. *Journal of Chemical Physics, 11(11),* 512–520.
20. Hong, H., He, H., Jia, D., Zhang, H. (2011). Effect of wood flour on the curing behavior, mechanical properties, and water absorption of natural rubber/wood flour composites. *Journal of Macromolecular Science, Part B, 50(8),* 1625–1636. DOI 10.1080/00222348.2010.541006.
21. Ishak, Z. M., Bakar, A. A. (1995). An investigation on the potential of rice husk ash as fillers for epoxidized natural rubber (ENR). *European Polymer Journal, 31(3),* 259–269. DOI 10.1016/0014-3057(94)00156-1.
22. Ismail, H., Norjulia, A. M., Ahmad, Z. (2010). The effects of untreated and treated kenaf loading on the properties of kenaf fibre-filled natural rubber compounds. *Polymer-Plastics Technology and Engineering, 49(5),* 519–524. DOI 10.1080/03602550903283117.
23. Kim, W., Argento, A., Lee, E., Flanigan, C., Houston, D. et al. (2012). High strain-rate behavior of natural fiber-reinforced polymer composites. *Journal of Composite Materials, 46(9),* 1051–1065. DOI 10.1177/0021998311414946.
24. Afiratul, A. A., Noriman, N. Z., Husin, K., Sam, S. T., Ismail, H. et al. (2015). The Addition of imperata cylindrica as natural filler in epoxidized natural rubber filled recycled nitrile glove: Cure characteristics and physical properties. *Applied Mechanics and Materials, 815,* 39–43. Trans Tech Publications Ltd.
25. Vijay, R., Singaravelu, D. L. (2016). Experimental investigation on the mechanical properties of Cyperus pangorei fibers and jute fiber-based natural fiber composites. *International Journal of Polymer Analysis and Characterization, 21(7),* 617–627. DOI 10.1080/1023666X.2016.1192354.
26. Santiagoo, R., Ismail, H., Hussin, K. (2011). Mechanical properties, water absorption, and swelling behaviour of rice husk powder filled polypropylene/recycled acrylonitrile butadiene rubber (PP/NBRr/RHP) biocomposites using silane as a coupling agent. *BioResources, 6(4),* 3714–3726.
27. Ismail, H., Ragunathan, S., Hussin, K. (2011). Tensile properties, swelling, and water absorption behavior of rice-husk-powder-filled polypropylene/(recycled acrylonitrile-butadiene rubber) composites. *Journal of Vinyl and Additive Technology, 17(3),* 190–197. DOI 10.1002/vnl.20261.
28. Zabihzadeh, S. M. (2010). Water uptake and flexural properties of natural filler/HDPE composites. *BioResources, 5 (1),* 316–232.
29. Dahham, O. S., Noriman, N. Z., Sam, S. T., Rosniza, H., Marwa, N. A. S. et al. (2016). The effects of trans-polyoctylene rubber (TOR) as a compatibilizer on the properties of epoxidized natural rubber/recycled silicone catheter (ENR-25/rSC) vulcanizate. *MATEC Web of Conferences, 78,* 01076. EDP Sciences.
30. Raju, G., Haris, M. R. H. M. (2016). Preparation and characterization of acidified chitosan immobilized in epoxidized natural rubber. *Polymer Testing, 53,* 1–6. DOI 10.1016/j.polymertesting.2016.05.005.

31. Dahham, O. S., Noriman, N. Z., Sam, S. T., Ismail, H., Ragunathan, S. et al. (2016). Properties of recycled natural latex gloves filled NBR: Effects of sawdust and trans polyoctylene rubber. *Journal of Polymer Materials, 33(4),* 647.
32. Zhu, Z., Ye, C., Fu, W., Wu, H. (2016). Improvement in mechanical and thermal properties of polylactic acid biocomposites due to the addition of hybrid sisal fibers and diatomite particles. *International Journal of Polymer Analysis and Characterization, 21(5),* 365–377. DOI 10.1080/1023666X.2016.1160529.
33. Zulkepli, N. N., Ismail, H. (2012). A study of FTIR, thermal properties and natural weathering test on NBRvirgin/recycled with SBR blends. *Polymer-Plastics Technology and Engineering, 51(4),* 350–357. DOI 10.1080/03602559.2011.639324.